Monis et al., https://doi.org/10.1083/jcb.201611138

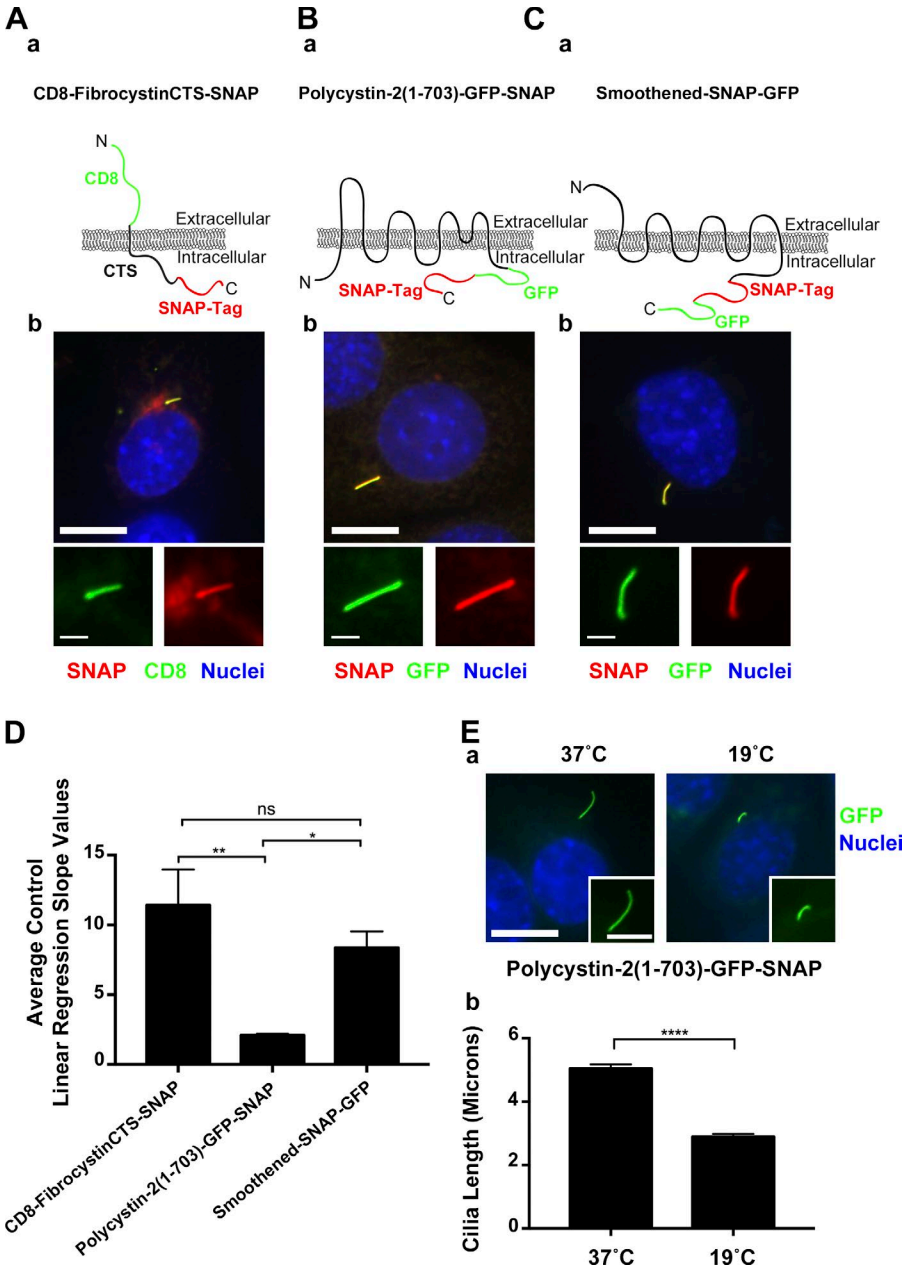

Figure S1. **Ciliary membrane protein constructs, trafficking rates, and cilia length after temperature shift to 19°C.** (A) HsCD8-MmFibrocystinCTS-SNAP (WJM8). (Aa) This construct contains part of the extracellular domain, the single transmembrane domain, and entire ciliary targeting sequence of MmFibrocystin. The extracellular N-terminal HsCD8 tag is used as an epitope marker and to maintain proper membrane protein topology. (Ab) IMCD3 Flp-In cells expressing ciliary localized CD8-fibrocystinCTS-SNAP stained with SNAP TMR STAR (red), CD8 antibody (green), and nuclei detected with DAPI (blue). Bars, 10 µm. Insets are 235% enlargements of the cilia. (B) HsPolycystin-2(1-703)-GFP-SNAP (WJM15). (Ba) This construct is truncated after amino acid 703 and is missing the ER-retention signal on its C-terminal end. (Bb) IMCD3 Flp-In cells expressing ciliary localized polycystin-2(1-703)-GFP-SNAP stained with SNAP TMR STAR (red), GFP (green), and nuclei detected with DAPI (blue). Bars, 10 µm. (C) MmSmoothened-SNAP-GFP (WJM6). (Ca) This construct contains the full-length amino acid sequence of MmSmoothened. (Cb) IMCD3 Flp-In cells expressing ciliary localized smoothened-SNAP-GFP stained with SNAP TMR STAR (red), GFP (green) and nuclei detected with DAPI (blue). Bars, 10 µm. (D) Mean control linear regression slope values for CD8-fibrocystinCTS-SNAP, polycystin-2(1-703)-GFP-SNAP, and smoothened-SNAP-GFP from Fig. 2 (n = 6 control slope values per membrane protein). Data were analyzed using one-way ANOVA and Tukey's multiple-comparison test. *, $P < 0.05$; **, $P < 0.01$. (E) Temperature of 19°C causes cilia to shorten. (Ea) Polycystin-2-GFP-SNAP IMCD Flp-In cells incubated at either 37°C or for 2 h at 19°C. GFP (green) and nuclei detected with DAPI (blue). Bars, 10 µm. Insets are 150% enlargements of the cilia. (Eb) Cilia incubated at 19°C are shorter compared with control (n = 100 cilia). Data were analyzed using the unpaired Student's t test. ****, $P < 0.0001$. Error bars represent SEM.

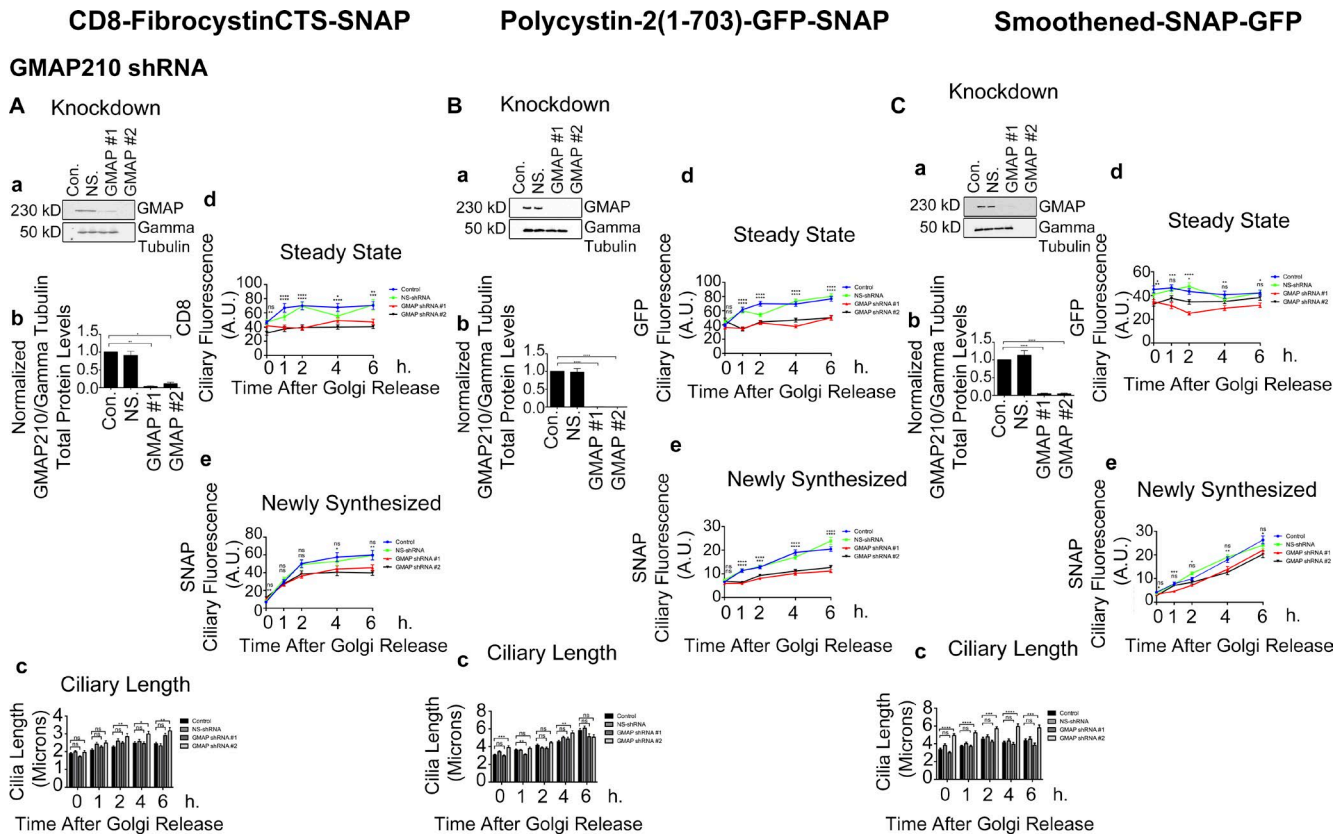

Figure S2. **GMAP210 knockdown strongly affects fibrocystin and polycystin-2 ciliary trafficking but only modestly affects smoothened trafficking to the primary cilium.** (A) Quantification of CD8-fibrocystinCTS-SNAP, (B) polycystin-2(1-703)-GFP-SNAP, and (C) smoothened-SNAP-GFP trafficking from the Golgi apparatus to the primary cilium during lenti-shRNA knockdown of GMAP210. (A–C, subpanel a) Selected immunoblot images of GMAP210 knockdown and γ tubulin loading control. (A–C, subpanel b) Quantification of knockdown. Mean protein levels plotted from three independent experiments for each condition (control, NS-shRNA, shRNA#1, and shRNA#2) and normalized to their corresponding γ tubulin loading control. shRNA-mediated knockdown of GMAP210 results in >90% reduction of total protein abundance. (A–C, subpanel c) Mean cilia length, (A–C, subpanel d) mean CD8 or GFP ciliary fluorescence, and (A–C, subpanel e) mean SNAP ciliary fluorescence plotted from three independent experiments in which 30 cilia were quantified for each condition (control, NS-shRNA, shRNA#1, and shRNA#2) at each time point (n = 90 total cilia per time point). CD8 or GFP and SNAP pixel intensity measurements were taken at individual time points starting at the time of temperature shift from 19°C to 37°C (0 h). Data were analyzed using one-way ANOVA and the Bonferroni multiple-comparisons test. The control condition was compared with shRNA#1 and shRNA#2 conditions to determine statistical significance. *, P < 0.05; **, P < 0.01; ***, P < 0.001; ****, P < 0.0001. Error bars represent SEM.

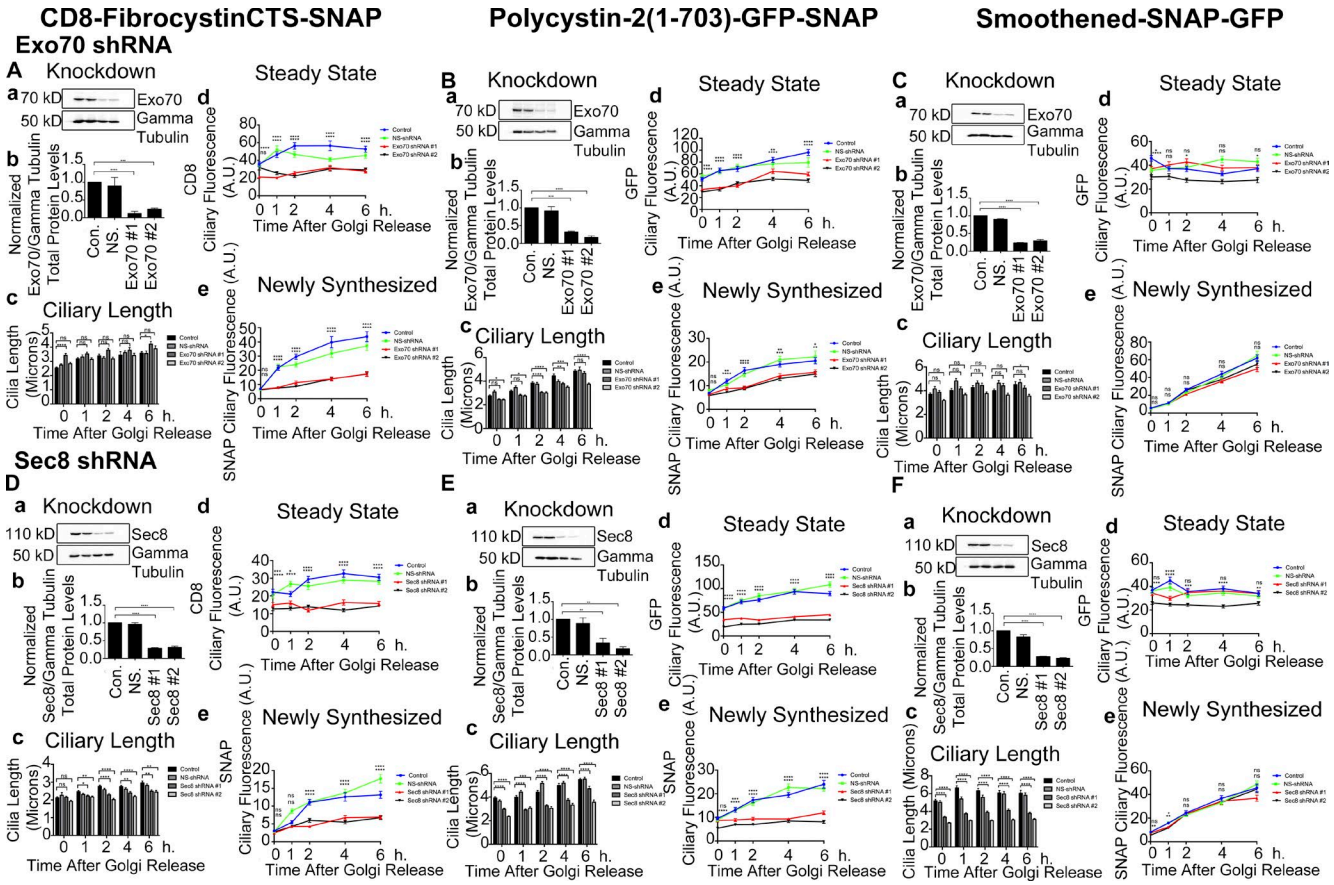

Figure S3. **Exocyst knockdown affects fibrocystin and polycystin-2 but not smoothened trafficking to the primary cilium.** Quantification of CD8-fibrocystinCTS-SNAP (A and D), polycstin-2(1-703)-GFP-SNAP (B and E), and smoothened-SNAP-GFP (C and F) trafficking from the Golgi apparatus to the primary cilium during lenti-shRNA knockdown of either Exo70 or Sec8. (A–F, subpanel a) Selected immunoblot images of either Exo70 or Sec8 knockdown and γ tubulin loading control. (A–F, subpanel b) Quantification of knockdown. Mean protein levels plotted from three independent experiments for each condition (control, NS-shRNA, shRNA#1, and shRNA#2) and normalized to their corresponding γ tubulin loading control. shRNA-mediated knockdown of either Exo70 or Sec8 results in 80%–90% reduction of total protein abundance. (A–F, subpanel c) Mean cilia length, (A–F, subpanel d) mean CD8 or GFP ciliary fluorescence, and (A–F, subpanel e) mean SNAP ciliary fluorescence plotted from three independent experiments in which 30 cilia were quantified for each condition (control, NS-shRNA, shRNA#1, and shRNA#2) at each time point (n = 90 total cilia per time point). CD8 or GFP and SNAP pixel intensity measurements were taken at individual time points starting at the time of temperature shift from 19°C to 37°C (0 h). Data were analyzed using one-way ANOVA and the Bonferroni multiple-comparisons test. The control condition was compared with the shRNA#1 and shRNA#2 conditions to determine statistical significance. *, P < 0.05; **, P < 0.01; ***, P < 0.001; ****, P < 0.0001. Error bars represent SEM.

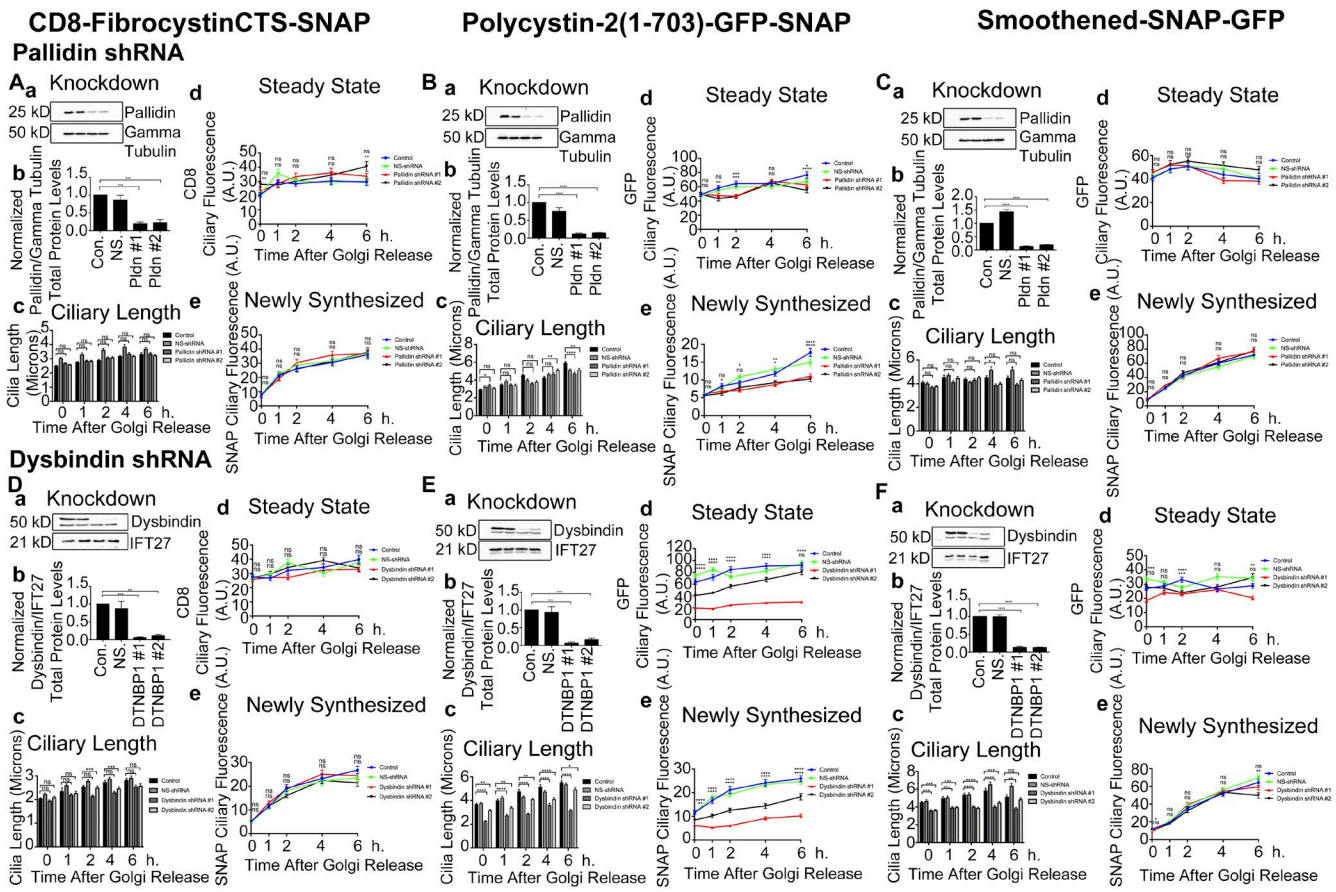

Figure S4. **BLOC-1 knockdown affects polycystin-2 but not fibrocystin or smoothened trafficking to the primary cilium.** Quantification of (A and D) CD8-fibrocystinCTS-SNAP, (B and E) polycstin-2(1-703)-GFP-SNAP, and (C and F) smoothened-SNAP-GFP trafficking from the Golgi apparatus to the primary cilium during lenti-shRNA knockdown of either pallidin or dysbindin. (A–F, subpanel a) Selected immunoblot images of pallidin or dysbindin knockdown and either γ tubulin or IFT27 loading control. (A–F, subpanel b) Quantification of knockdown. Mean protein levels plotted from three independent experiments for each condition (control, NS-shRNA, shRNA#1, and shRNA#2) and normalized to their corresponding γ tubulin or IFT27 loading control. shRNA-mediated knockdown of either pallidin or dysbindin results in >90% reduction of total protein abundance. (A–F, subpanel c) Mean cilia length, (A–F, subpanel d) mean CD8 or GFP ciliary fluorescence, and (A–F, subpanel e) mean SNAP ciliary fluorescence plotted from three independent experiments in which 30 cilia were quantified for each condition (control, NS-shRNA, shRNA#1, and shRNA#2) at each time point (n = 90 total cilia per time point). CD8 or GFP and SNAP pixel intensity measurements were taken at individual time points starting at the time of temperature shift from 19°C to 37°C (0 h). Data were analyzed using one-way ANOVA and the Bonferroni multiple-comparisons test. The control condition was compared with the shRNA#1 and shRNA#2 conditions to determine statistical significance. *, P < 0.05; **, P < 0.01; ***, P < 0.001; ****, P < 0.0001. Error bars represent SEM.

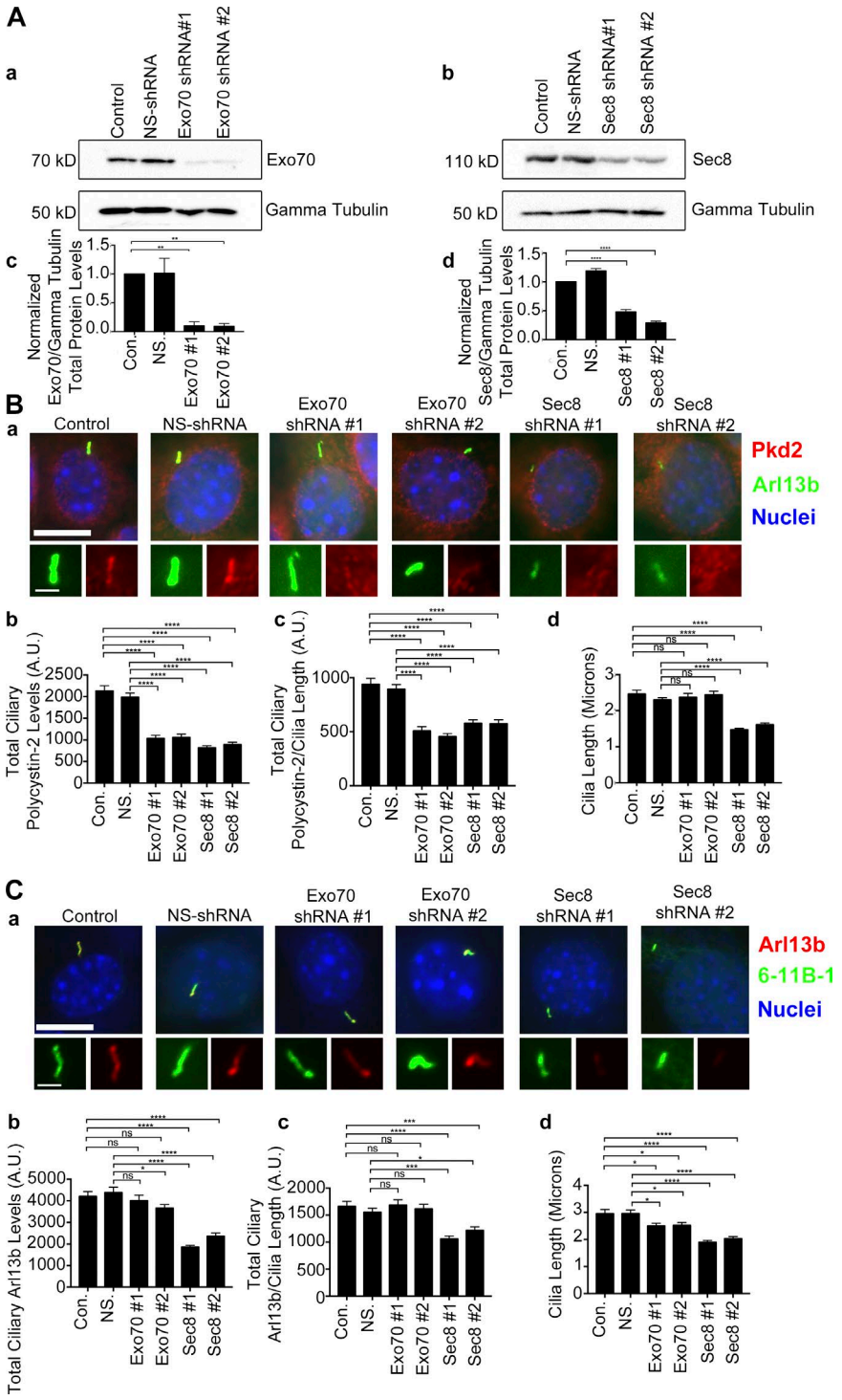

Figure S5. **Exo70 and Sec8 knockdown decreases endogenous ciliary polycystin-2 levels.** (A) Immunoblot and quantification of total protein levels of MEK cells expressing either Exo70 or Sec8 lenti-shRNAs. Selected immunoblot images showing (Aa) Exo70 knockdown and (Ab) Sec8 knockdown with γ tubulin loading control. Quantification of (Ac) Exo70 mean protein levels and (Ad) Sec8 mean protein levels for each condition (control, NS-shRNA, shRNA#1, and shRNA#2) that are normalized to their corresponding γ tubulin loading control. shRNA-mediated knockdown of either Exo70 or Sec8 results in >80% reduction of total protein abundance. (B) Immunostaining and quantification of ciliary polycystin-2 and cilia length in MEK cells expressing either Exo70 or Sec8 lenti-shRNA. (Ba) Selected images of polycystin-2 (Pkd2) antibody staining (red), Arl13b staining (green), and nuclei are detected with DAPI (blue). Bars, 10 μm. Insets are 240% enlargements of the cilia. (Bb) Mean total ciliary polycystin-2 (Bc) and ciliary polycystin-2 per micrometer is reduced in cells expressing Exo70 or Sec8 lenti-shRNAs. (Bd) Mean cilia length is reduced in cells expressing Sec8 shRNAs. (C) Immunostaining and quantification of ciliary Arl13b and cilia length in MEK cells expressing either Exo70 or Sec8 lenti-shRNA. (Ca) Selected images of Arl13b antibody staining (red), acetylated tubulin (6-11B-1) antibody staining (green), and nuclei are detected with DAPI (blue). Bar, 10 μm. Insets are 240% enlargements of the cilia. (Cb) Mean steady-state ciliary Arl13b and (Cc) ciliary Arl13b per micrometer is reduced in cells expressing Sec8 lenti-shRNAs. (Cd) Mean ciliary assembly is reduced in cells expressing Sec8 shRNAs. n = 107 cilia per experimental group. Error bars are SEM. Data were analyzed using one-way ANOVA and the Bonferroni multiple-comparisons test. *, P < 0.05; **, P < 0.01; ***, P < 0.001; ****, P < 0.0001.

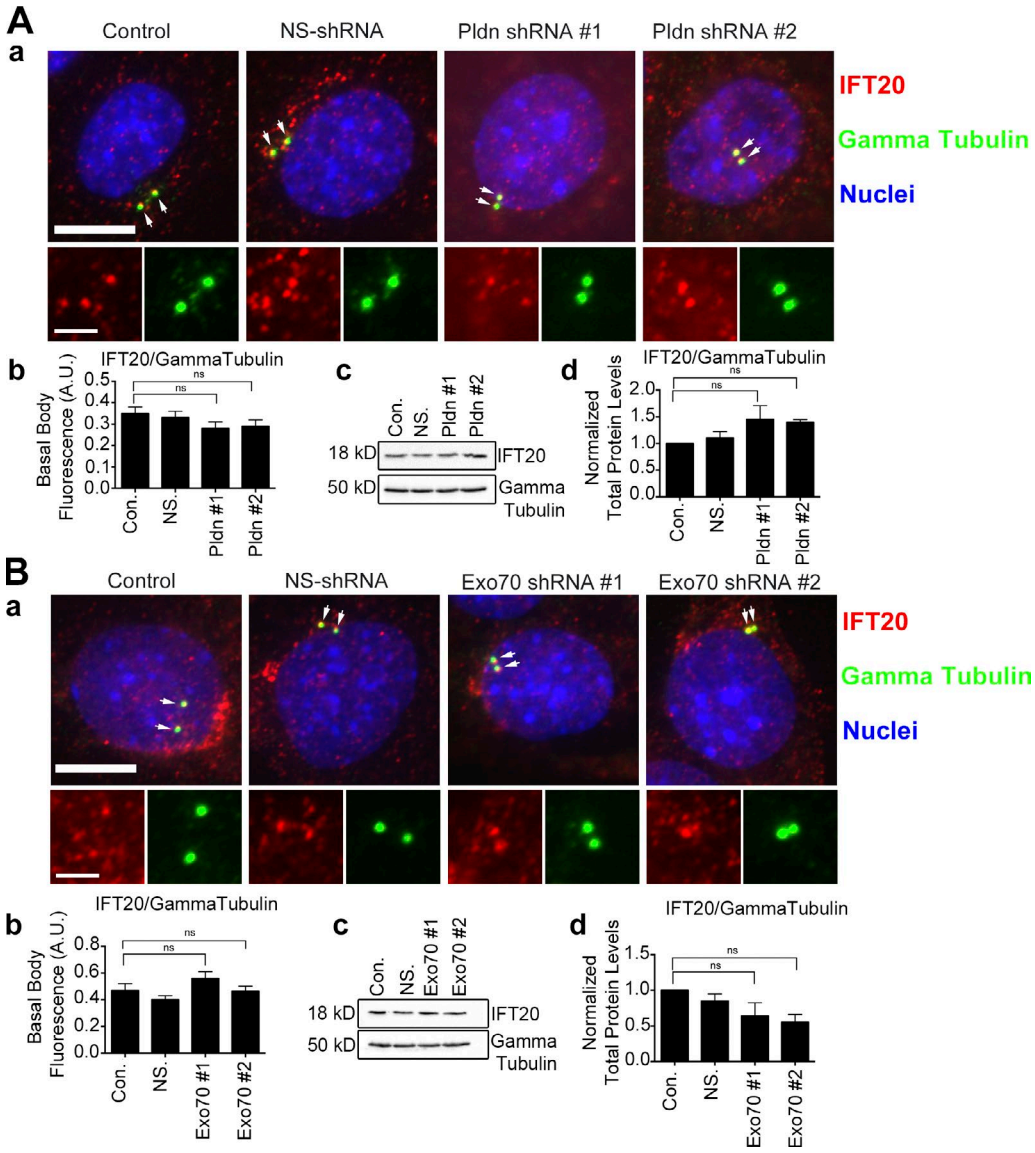

Figure S6. **IFT20 localization at the basal body is not affected by the knockdown of either pallidin or Exo70.** (A) Endogenous IFT20 levels at the basal body in CD8-fibrocystinCTS-SNAP Flp-In IMCD3 cells expressing either nonsilencing or pallidin lenti-shRNAs. (Aa) Selected images showing IFT20 localization at the basal body (arrows). IFT20 antibody staining (red), γ tubulin antibody staining (green), and nuclei are detected with DAPI (blue). Bars, 10 µm. Insets are 185% enlargements of the centrosome regions. (Ab) No difference in the mean steady-state levels of IFT20 at the basal body in the pallidin knockdown cells compared with the control. (Ac) Selected immunoblot images of total endogenous IFT20 and γ tubulin loading control protein levels. (Ad) No difference in the mean total protein levels of IFT20 in the pallidin knockdown cells compared with the control. (B) Endogenous IFT20 levels at the basal body in CD8-fibrocystinCTS-SNAP Flp-In IMCD3 cells expressing either nonsilencing or Exo70 lenti-shRNAs. (Ba) Selected images showing IFT20 localization at the basal body (arrows). IFT20 antibody staining (red), γ tubulin antibody staining (green), and nuclei are detected with DAPI (blue). Bar, 10 µm. Insets are 185% enlargements of the centrosome regions. (Bb) No difference in the mean steady-state levels of IFT20 at the basal body in the Exo70 knockdown cells compared with the control. (Bc) Selected immunoblot images of total endogenous IFT20 and γ tubulin loading control protein levels. (Bd) No difference in the mean total protein levels of IFT20 in the Exo70 knockdown cells compared with the control. *n* = 50 basal bodies per experimental group. Error bars are SEM. Data were analyzed using one-way ANOVA and the Bonferroni multiple-comparisons test.

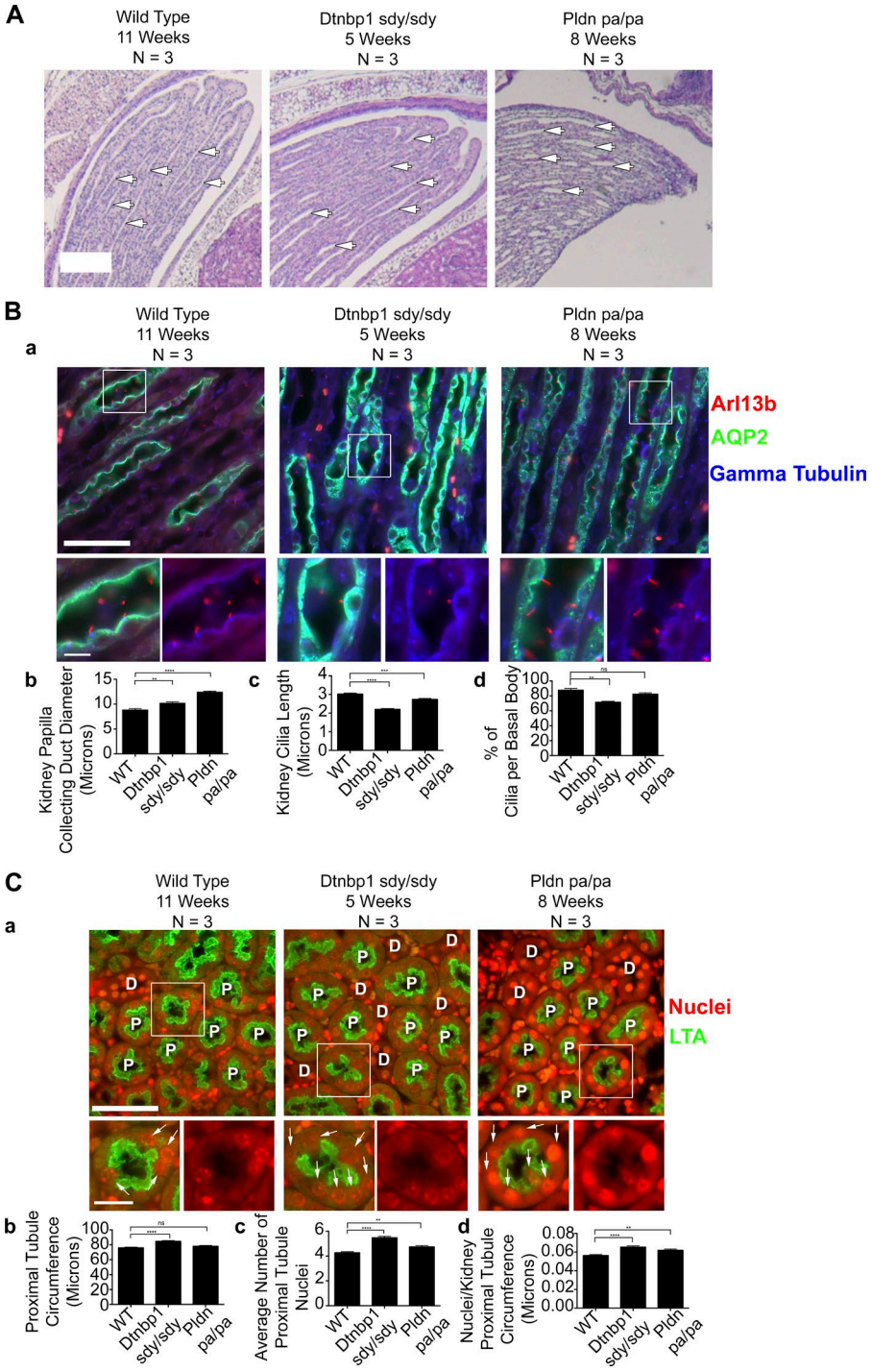

Figure S7. **Young *Dtnbp1*$^{sdy/sdy}$ and *Pldn*$^{pa/pa}$ mice have mildly cystic kidneys.** (A) Hematoxylin and eosin staining of mouse kidney papillae of wild-type (11 wk of age), *Dtnbp1*$^{sdy/sdy}$ (5 wk of age), and *Pldn*$^{pa/pa}$ (8 wk of age). Bar, 200 µm. (B) Immunohistochemistry and diameter quantification of wild-type, *Dtnbp1*$^{sdy/sdy}$, and *Pldn*$^{pa/pa}$ kidney collecting ducts. (Ba) Selected images of mouse kidney sections stained with cilia marker Arl13b antibody (red), collecting duct marker AQP2 antibody (green), and basal body marker γ tubulin antibody (blue). Bars, 50 µm. Insets are 250% enlargements. (Bb) Mean collecting duct diameter is increased in *Dtnbp1*$^{sdy/sdy}$ and *Pldn*$^{pa/pa}$ kidneys (n = 198 collecting ducts per group). (Bc) Mean cilia assembly is reduced in the *Dtnbp1*$^{sdy/sdy}$ and *Pldn*$^{pa/pa}$ kidneys (n = 300 cilia per group) and (Bd) the percentage of cilia per basal body is reduced *Dtnbp1*$^{sdy/sdy}$ kidneys (n = 300 basal bodies per group). (C) Immunohistochemistry, tubule circumference quantification, mean number of tubule nuclei, and nuclei per tubule circumference of wild-type, *Dtnbp1*$^{sdy/sdy}$, and *Pldn*$^{pa/pa}$ kidney proximal tubules. (Ca) Selected images of mouse kidney sections stained with proximal tubule marker LTA (green) and nuclei Dapi (red). Most tubules are proximal, and some are marked with "P." The few distal convoluted tubules are marked with "D." Arrows indicate proximal tubule nuclei. Bar, 50 µm. Insets are 175% enlargements. (Cb) Mean proximal tubule circumference is increased in *Dtnbp1*$^{sdy/sdy}$ kidneys, (Cc) the mean number of proximal tubule nuclei in the *Dtnbp1*$^{sdy/sdy}$ and *Pldn*$^{pa/pa}$ kidneys is increased, and (Cd) the nuclei/kidney proximal tubule circumference in the *Dtnbp1*$^{sdy/sdy}$ and *Pldn*$^{pa/pa}$ kidneys is increased (n = 96 proximal tubules per group). n = 3 mice per experimental group. Error bars are SEM. Data were analyzed using one-way ANOVA and the Bonferroni multiple-comparisons test. **, P < 0.01; ***, P < 0.001; ****, P < 0.0001.

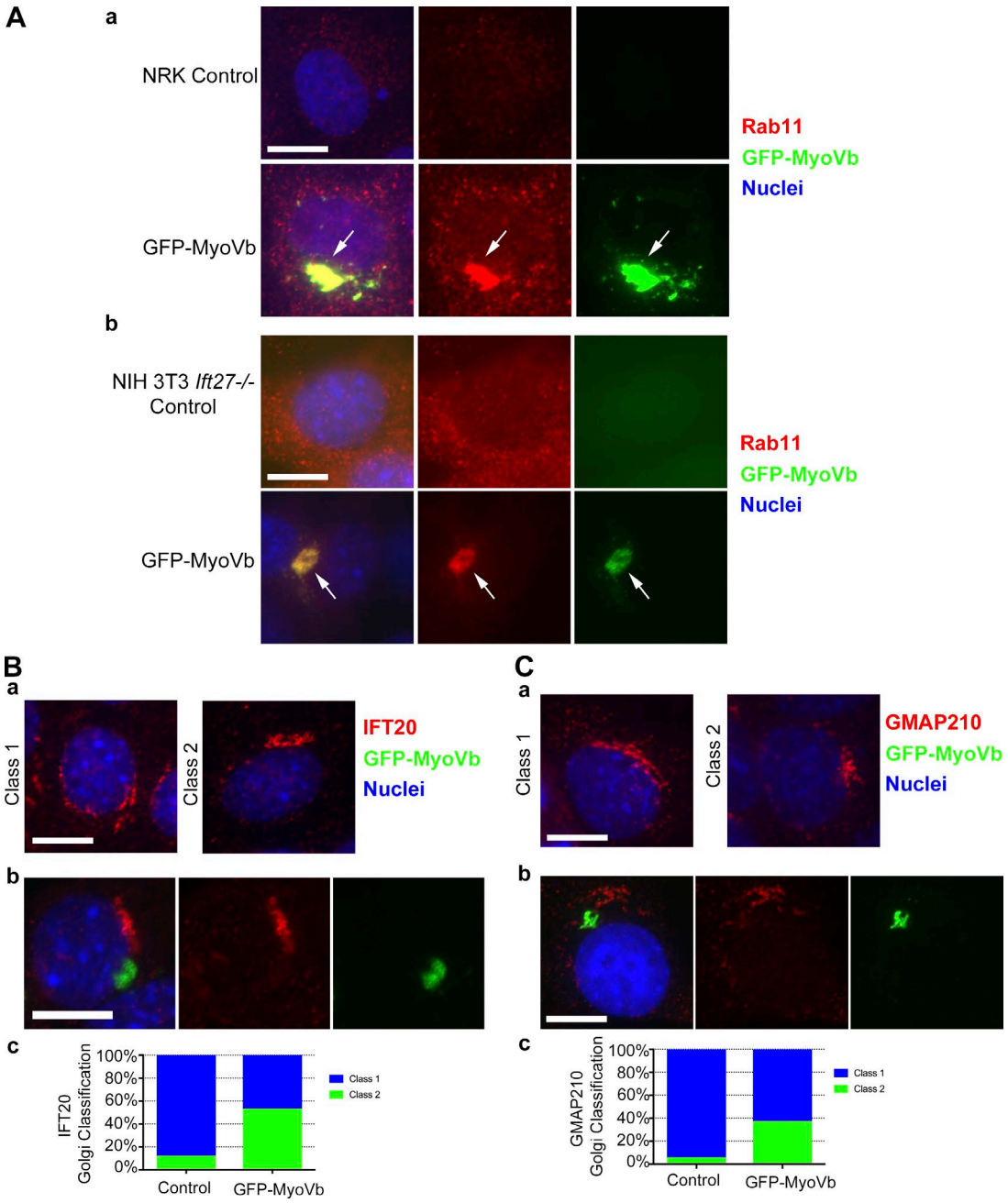

Figure S8. **GFP-MyoVb colocalizes with the recycling endosome marker Rab11 and induces compaction of the Golgi complex.** (A) NRK and NIH 3T3 *Ift27*$^{-/-}$ cells expressing GFP-MyoVb C-terminal tail. (Aa) Selected images of NRK control and GFP-MyoVb-expressing cells stained with Rab11 antibody (red), GFP-MyoVb (green), and nuclei detected with DAPI (blue). Bar, 10 µm. (Ab) Selected images of NIH 3T3 *Ift27*$^{-/-}$ control and GFP-MyoVb-expressing cells stained with Rab11 antibody (red), GFP-MyoVb (green), and nuclei detected with DAPI (blue). Bar, 10 µm. GFP-MyoVb colocalizes with the recycling endosome marker Rab11 (arrows). (B and C) Golgi classification and GFP-MyoVb expression induces Golgi compaction. (Ba) Selected images of IMCD3 cells stained with IFT20 antibody (red) and nuclei detected with DAPI (blue) or (Ca) GMAP210 antibody (red) and nuclei detected with DAPI (blue). Class 1: cells with noncompact Golgi around the nucleus. Class 2: cells with compact Golgi. Bars, 10 µm. (Bb) Selected images of IMCD3 cells stained with IFT20 antibody (red), GFP-MyoVb (green), and nuclei detected with DAPI (blue). GFP-MyoVb does not colocalize with IFT20 at the Golgi. Bar, 10 µm. (Cb) Selected images of IMCD3 cells stained with GMAP210 antibody (red), GFP-MyoVb (green), and nuclei detected with DAPI (blue). GFP-MyoVb does not colocalize with GMAP210 at the Golgi. Bar, 10 µm. (Bc and Cc) GFP-MyoVb expression induces compaction of the Golgi complex. *n* = 95 cells per experimental group.

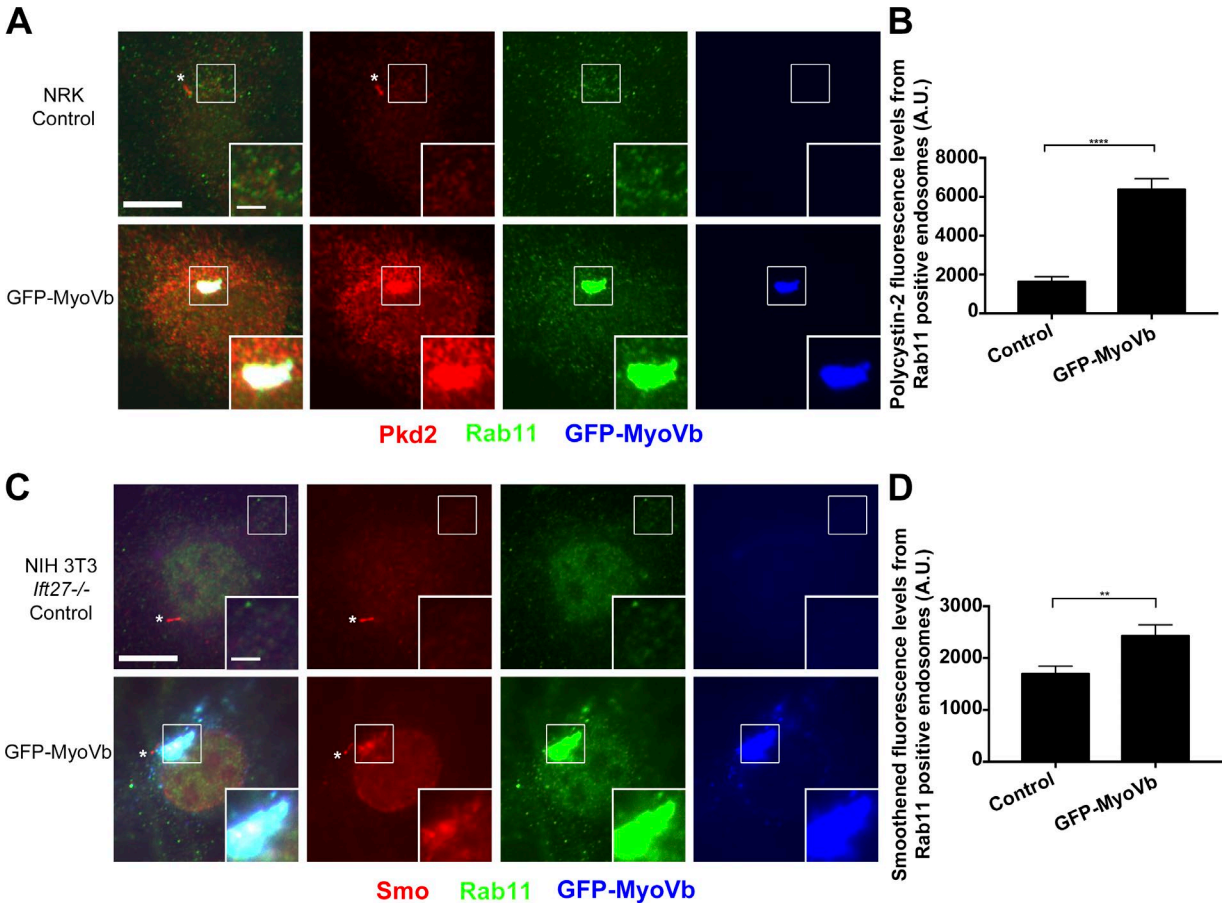

Figure S9. **Polycystin-2 and smoothened accumulate in Rab11-positive endosomes when GFP-MyoVb is expressed.** (A) Selected images of NRK control and GFP-MyoVb-expressing cells stained with polycystin-2 (Pkd2) antibody (red), Rab11 antibody (green), and GFP-MyoVb (blue). A cilium positive for polycystin-2 is marked by an asterisk in the NRK control. Note the bolus accumulation of polycystin-2 in Rab11-positive endosomes and the lack of ciliary polycystin-2 staining when GFP-MyoVb is expressed. Insets are 200% enlargements of Rab11-positive endosomes. Bars, 10 µm. (B) Quantification of mean polycystin-2 fluorescence levels from Rab11-positive endosomes. There is a significant accumulation of polycystin-2 in Rab11-positive endosomes when GFP-MyoVb is expressed. $n = 55$ Rab11-positive endosome puncta groups. (C) Selected images of NIH 3T3 *Ift27*$^{-/-}$ and GFP-MyoVb-expressing cells stained with smoothened (Smo) antibody (red), Rab11 antibody (green), and GFP-MyoVb (blue). Cilia positive for smoothened are marked by asterisks in the NIH 3T3 *Ift27*$^{-/-}$ control and GFP-MyoVb-expressing cells. Note the minimal accumulation of smoothened in Rab11-positive endosomes and the presence of ciliary smoothened staining in the GFP-MyoVb-expressing cells. Insets are 200% enlargements of Rab11-positive endosomes. Bars, 10 µm. (D) Quantification of mean smoothened fluorescence levels from Rab11-positive endosomes. There is a minimal yet significant accumulation of smoothened in Rab11-positive endosomes when GFP-MyoVb is expressed. $n = 55$ Rab11-positive endosome puncta groups. Error bars are SEM. Data were analyzed with the unpaired Student's *t* test. **, $P < 0.01$; ****, $P < 0.0001$.

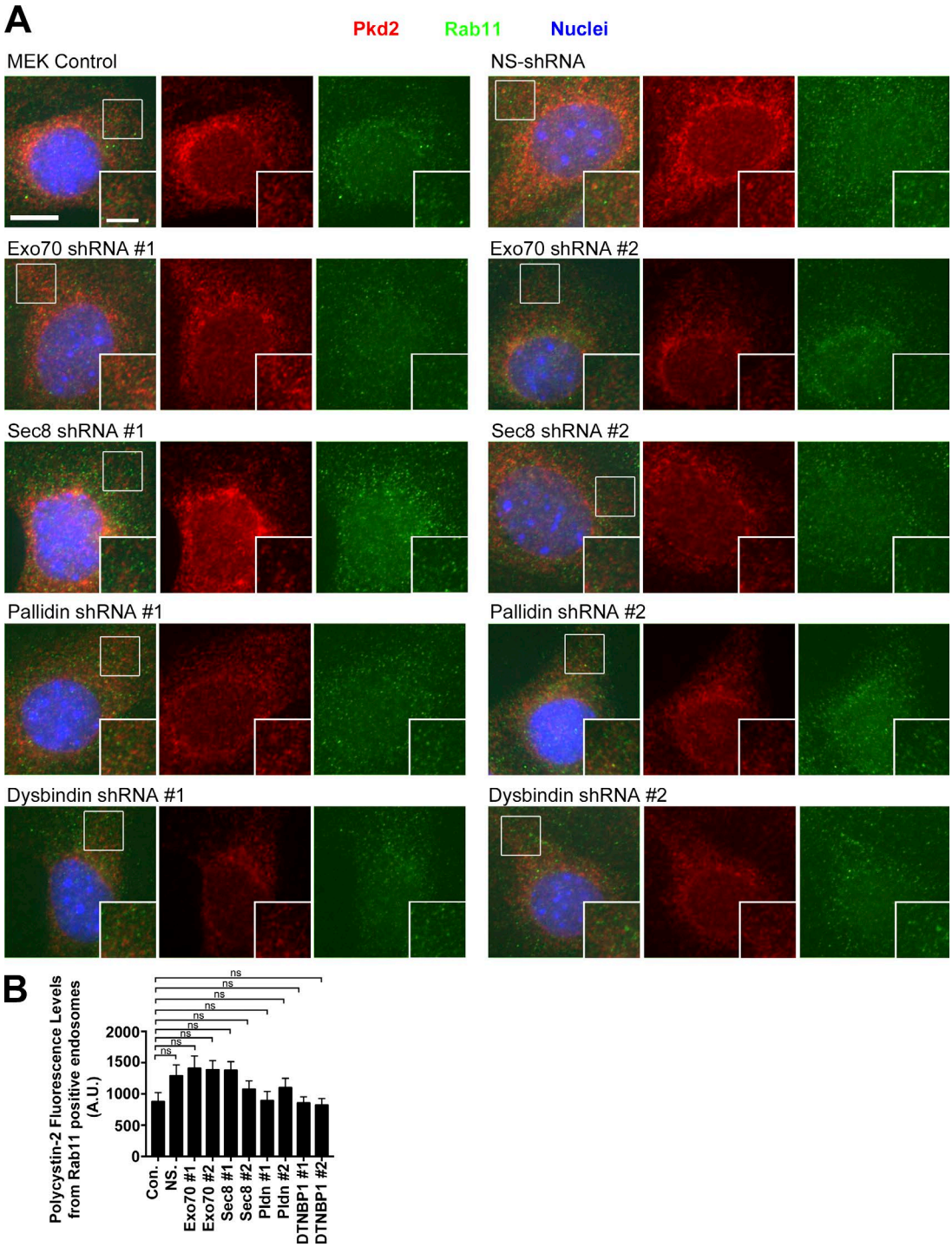

Figure S10. **Polycystin-2 is not detected in Rab11-positive endosomes when either the exocyst or BLOC-1 is knocked down.** (A) Selected images of MEK control, NS-shRNA, Exo70 shRNA #1, Exo70 shRNA #2, Sec8 shRNA #1, Sec8 shRNA #2, pallidin shRNA #1, pallidin shRNA #2, dysbindin shRNA #1, and dysbindin shRNA #2 cells stained with polycystin-2 (Pkd2) antibody (red), Rab11 antibody (green), and nuclei detected with DAPI (blue). Bars, 10 µm. Insets are 150% enlargements of Rab11-positive endosomes. (B) Quantification of mean polycystin-2 fluorescence levels from Rab11-positive endosomes. There is no statistical difference between the control and experimental groups. *n* = 50 Rab11-positive endosome puncta groups. Error bars are SEM. Data were analyzed using one-way ANOVA and the Bonferroni multiple-comparisons test.

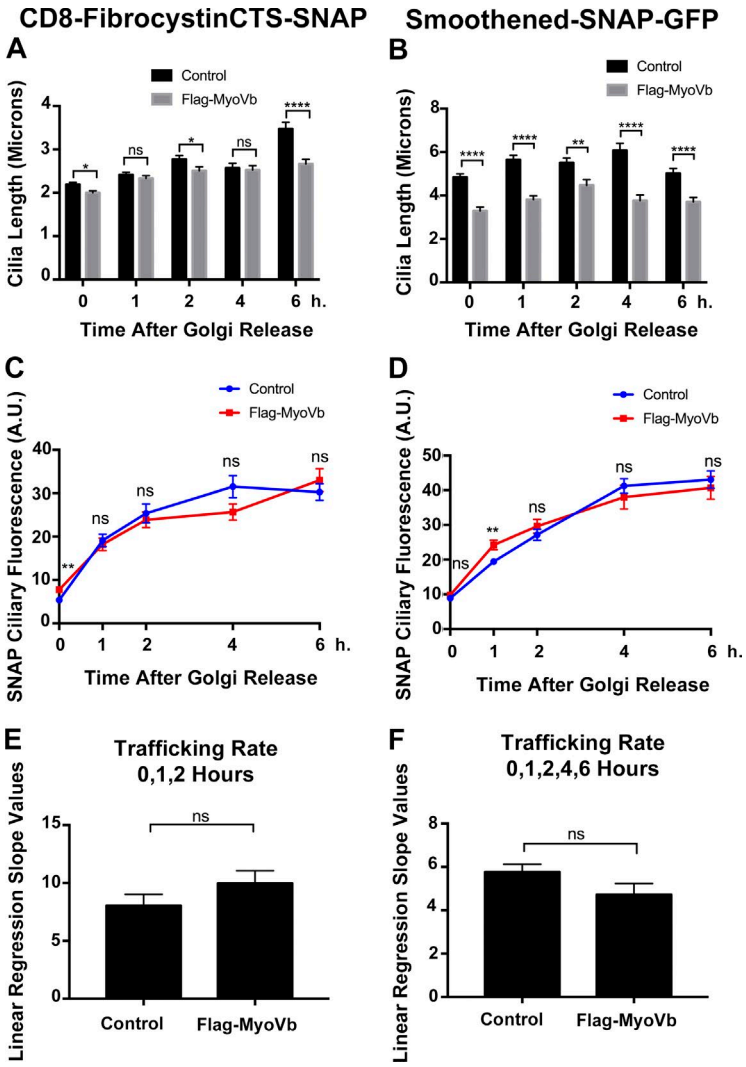

Figure S11. **Overexpression of MyoVb-GFP does not perturb fibrocystin or smoothened trafficking to the primary cilium.** (A) Mean cilia length of CD8-fibrocystinCTS-SNAP and (B) smoothened-SNAP-GFP IMCD Flp-In control and Flag-MyoVb-expressing cells after Golgi release. (C) Mean SNAP ciliary fluorescence of CD8-fibrocystinCTS-SNAP and (D) smoothened-SNAP-GFP delivery to the cilium in IMCD Flp-In control and Flag-MyoVb-expressing cells after Golgi release. The mean SNAP ciliary fluorescence and ciliary length were plotted from three independent experiments in which 30 cilia were quantified for each condition (control and Flag-MyoVb) at each time point (n = 90 total cilia per time point). (E) Linear regression slope values of newly synthesized CD8-fibrocystinCTS-SNAP and (F) smoothened-SNAP-GFP in IMCD Flp-In control and Flag-MyoVb-expressing cells after Golgi release at either 0, 1, or 2 h or 0, 1, 2, 4, or 6 h. Slope values between control and Flag-MyoVb groups were compared with one another to determine statistical significance. Error bars represent SEM. Data were analyzed using the unpaired Student's t test. *, $P < 0.05$; **, $P < 0.01$; ****, $P < 0.0001$.